An Efficient Ring-Shaped Electromagnetic Thruster

Daniele Funaro, Alessandro Chiolerio

An Efficient Ring-Shaped Electromagnetic Thruster

Daniele Funaro
Dipartimento di Scienze Chimiche e Geologiche
Università di Modena e Reggio Emilia
Via Campi 103, 41125 Modena (Italy)
daniele.funaro@unimore.it

Alessandro Chiolerio
Istituto Italiano di Tecnologia,
Center for Converging Technologies, Soft Bioinspired Robotics
Via Morego 30, 16165 Genova (Italy)
alessandro.chiolerio@iit.it

Abstract

An electromagnetic thruster (EMT) is proposed and tested with success. Its design is inspired by theoretical considerations whose predictions well match with the experimental findings. The efficiency is superior to any other device so far reported in literature, producing a directional thrust of approximately $2.7 \times 10^{-5} M$ Newtons/Kg, where M denotes the mass of the thruster itself, with an injected power of approximately 10 Watts. The prototype has the shape of a ring and is supplied with both radio-frequency signals and a stationary high voltage. Improvements and generalizations can be easily devised by adjusting the geometry of the device.

Keywords: Electromagnetic thruster, radio frequency, high voltage, vortex ring.

1 Background

Cavity thrusters use radio frequencies (RF) as the sole way to generate thrust, justifying therefore the name electromagnetic thrusters (EMTs). The *EmDrive* [1] is a truncated conical resonant cavity claimed to produce thrust in the direction of the largest base when supplied at the interior with electromagnetic waves of the proper intensity. The thrust results from the difference in radiation pressure, due to the asymmetry of the device. Other geometries were successively tested, such as for instance the *Cannae Drive*. Some research groups actually measured the presence of a very small thrust in their tests, but the same experiments conducted by other authors did not confirm the outcomes. Indeed, since the forces were too small, they could have been explained by the interference of thermal effects or by the action of the environmental (Earth's) magnetic field.

A detailed discussion with a wide list references is found in *Wikipedia*. Updated information is also available in [2].

In truth, these devices violate the law of conservation of momentum. An explanation is that an EMT operates by transferring momentum to the so called *quantum vacuum* [3], [4], [5]. Indeed, the *zero-point energy* is the lowest possible energy state assumed by a quantum mechanical system. Such radiation is of electromagnetic nature and pervades the universe. A typical quantum manifestation is the Casimir effect, where two parallel uncharged metal plates kept at a suitable distance are subject to an attractive force [6]. Such a phenomenon is extremely mild and is usually explained by arguing that the vacuum energy at the exterior of the plates is larger than that trapped in between, resulting in a gradient of pressure acting on the surfaces.

A similar area of interest concerns asymmetrical capacitors, also known as *lifters*. When the device is charged, the two conductors tend to attract each other with a non zero resultant (Biefeld-Brown effect). In this fashion, the entire setting is subject to side acceleration. The so-called *anti-gravity flying machines* are very light capacitors immersed in a dielectric (air, for instance). They are charged with a potential difference of the order of tens of kVolts. Due to their asymmetry, the devices start rising and freely floating [7]. The official explanation relies on the fact that there is ionic wind production, due to a corona type effect. The asymmetric movement in air of such ions would be responsible for the thrust. These arguments are however not definitively convincing, since some devices seem to work also when the two plates of the capacitor are embedded in a solid dielectric material. We make reference to the review paper [8], containing a useful list of references and the history of the U.S. Patents related to the subject.

We are here proposing and characterizing a new EMT. Its design is suggested by theoretical considerations, and takes some inspiration from the abovementioned devices, by putting together all their peculiarities. In particular, we will take into consideration:

- The asymmetry of the device
- The supply of a RF in the range of 'resonance' of the device
- The addition of stationary high voltage electric fields
- The presence of a dielectric, possibly with high dielectric constant

The main issue relies on the following property. In the EmDrive the electromagnetic radiation is thrown in the cavity with very little control of what actually happens in there. In our prototype the wave is specifically driven around closed patterns. Due to the asymmetry of the paths, the device behaves like an 'unbalanced washing machine', spiraling towards a prescribed direction. Actually, a sort of 'friction', naturally occurring in the electromagnetic vacuum, should allow for the transfer of momentum from the device to the environment. More detailed comments are provided at the end of section 4.

2 Rotating electromagnetic waves

Maxwell's equations in vacuum, involving electric and magnetic fields ($\vec{E}$ and $\vec{B}$, respectively), read as follows:

$$\frac{\partial \vec{E}}{\partial t} = c^2 \mathrm{curl}\vec{B} \qquad \frac{\partial \vec{B}}{\partial t} = -\mathrm{curl}\vec{E} \qquad \mathrm{div}\vec{E} = 0 \qquad \mathrm{div}\vec{B} = 0 \qquad (2.1)$$

with c denoting the speed of light.

Peculiar solutions of the full set of equations, circulating in rounded cavities, are available in [9], [10], [11], [12]. For an infinitely long cylinder, exact expressions may be computed in terms of classical Bessel's functions. The magnetic field is distributed along the cylinder's axis, whereas the electric field assumes a dynamical distribution that simulates a rotation around the same axis. The simplest displacement is displayed in Fig. 1. In the picture, $\vec{B}$ is orthogonal to the page and periodically oscillates up and down. The figure rigidly rotates at uniform angular velocity. In this way, the electric field does not remain orthogonal to the direction of motion (in fact, it also displays a longitudinal component) and the entire electromagnetic wave does not travel at constant speed c, equal to that of light. This may sound atypical. On the other hand, it corresponds to what can be straightly recovered from resolving the set of equations in (2.1).

There are infinitely many solutions of this type. In the one shown in Fig. 1, the magnetic field vanishes (for any time) at the boundary of the cylinder. At the same boundary, the electric field is tangential to the boundary and oscillates according to a rule of the type $\sin(vt - \phi)$, where v is the peripheral speed of propagation and ϕ is the angle.

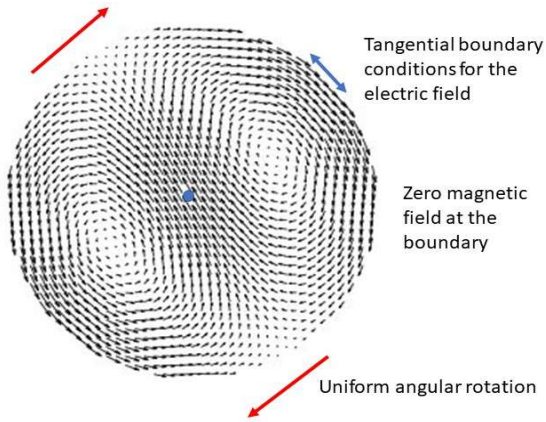

Figure 1: *Electric field displacement inside the section of the cylinder at a prescribed time. The picture rotates clockwise with constant angular speed.*

Practically, we should be able to get a similar evolution through a winding made of a conducting wire (solenoid) around a long cylinder of fixed diameter. Another straight conducting wire is placed along the axis (i.e., the one passing through the center of the disk in Fig. 1) and is connected to ground. The external wire is then supplied by alternate current. The signal is applied to an extreme, whereas the other is left free. This setting guarantees the rotation of the peripheral signal about the axis that consequently induces a special dynamical field distribution inside the cylinder. The right frequency to be applied depends on various factors, such as the composition of the cylinder, its diameter, and the conductivity constant of the external wire. The resonance of the spires of the outer winding is obtained when the generated magnetic field oscillates back and forth inside the cylinder in synchrony.

From the case of the cylinder one can easily pass to that of a ring (not necessarily of circular section) [13]. Here, exact solutions of (2.1) are not available, but can be computed numerically [14]. The evolution of the electric field now recalls that of fluid dynamic vortex rings [15], and the magnetic field circulates inside the body along closed lines.

3 Adding a stationary electric field

By suitably coupling Maxwell's equations with Euler's equation for non viscous fluids, one can obtain:

$$\frac{\partial \vec{E}}{\partial t} = c^2 \mathrm{curl}\vec{B} - \rho\vec{V} \qquad \frac{\partial \vec{B}}{\partial t} = -\mathrm{curl}\vec{E} \qquad \mathrm{div}\vec{B} = 0 \tag{3.1}$$

$$\rho\left(\mu^{-1}\frac{D\vec{V}}{Dt} + \vec{E} + \vec{V}\times\vec{B}\right) = -\epsilon_0^{-1}\vec{\nabla}p \tag{3.2}$$

with $\rho = \mathrm{div}\vec{E}$. These modeling equations were firstly introduced in [9]. Thus, we refer to that publication for explanations.

The first equation is the Ampère law, where $\vec{V}$ is a velocity field that describes the evolution of the electromagnetic information (not necessarily consisting of real massive charges, such as electrons). Moreover, the term $D\vec{V}/Dt$ is the substantial derivative, ϵ_0 is the dielectric constant in vacuum, and p is a potential denoting pressure density per unit of surface. Differently from fluid dynamics, p can also acquire negative values. Under the action of $\vec{\nabla}p$, a surface tends to shift in the direction of lower pressure.

Note also that the term $\vec{E} + \vec{V}\times\vec{B}$ recalls Lorentz's force. Finally, the constant μ is dimensionally equivalent to Coulomb/Kg. An estimation of μ in a very particular circumstance has been provided in [12], appendix H. If we enforce $\rho = 0$, we return to the set of equations (2.1) in vacuum. Therefore, the modeling equations (3.1)-(3.2) extend Maxwell's ones.

Exact rotating solutions on an infinite length cylinder can be calculated for ρ constant. It is enough to add linearly the solutions for $\rho = 0$ (see Section 2) to

the stationary one corresponding to a radial (with respect to the axis) electric field, as it happens inside a dielectric. In this way, a pressure p develops, that is the sum of a neat component and an oscillating one displaying zero average in a period of time. The situation is far more complex in the case of a ring, though it presents similar peculiarities.

In a real experiment, one has to take into account the dielectric constant of the body (cylinder, ring, or other more complicated structures). This has a significant role in the determination of the displacement of the fields. In fact, we expect that the angular speed of rotation (and the corresponding resonance frequency) varies with the dielectric properties. In order to know what happens inside the body, it is necessary at this level to rely on numerical computations.

It is not easy to figure out what is the balance of the terms in equation (3.2). This may vary depending on the sign of ρ. Moreover, some quantities grow linearly with the intensity of $\vec{E}$, whereas some others are quadratic. We skip at this stage a more accurate analysis.

For domains presenting a symmetry (as the cylinder with circular section) we have that, at any time instant, the integral of the pressure gradient is zero, so that we do not expect neat forces acting on the body. For non-symmetric domains we can draw some conclusions by considering what happens on their surface, though the analysis should be performed on the whole body.

4 Asymmetric rings

If we want to generate a non-vanishing resultant (i.e., the integral extended to the whole domain of the pressure gradient), it is necessary to work with an asymmetric body. We also want this resultant to be different from zero when averaged over a period of time. The practical example we have in mind is shown in Fig. 2.

Parametric elements are:

- The size of the entire device
- The ratio between the radii of the inner and outer diameters
- The section profile
- The composition of the dielectric

All these elements affect the resonance properties of the ring under the application of the RF signal. The limitations imposed to our device do not seem to be severely restrictive, anyway. Thus, there are possibilities for generalizations and improvements. The shape of the ring section should be however the primary concern.

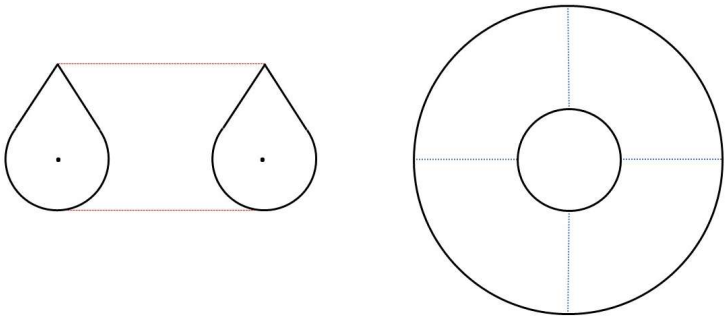

Figure 2: *Possible configuration of a ring with asymmetric section (left: section view; right: top view).*

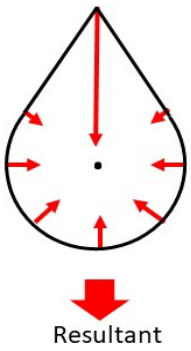

Figure 3: *Acceleration $D\vec{V}/Dt$ at the surface of the ring.*

A rough analysis conducted on the surface of the ring of Fig. 2 leads us to Fig. 3. For a rotating wave, a strong acceleration is produced on the top of the section, where the signal changes direction suddenly. If the section is well designed, we may conclude that there is a neat directional force acting on the body, and the verse of the resultant does not change with time.

One can argue at this point that we are violating the action-reaction principle. Besides the internal electromagnetic field there is an external one. The device in fact behaves as an antenna driven under resonance conditions, and we can suppose that a big deal of the energy is radiated outside. Due to the asymmetry, a slight unbalance is kept. We do not believe, however, that the amount of energy ejected can quantitatively explain the thrust.

In alternative, we can invoke the concept of vacuum, as done in other similar circumstances by other researchers. The ring is not only asymmetric because the top is different from the bottom, but also because a signal descending along

the internal side (the one corresponding to the hole) and ascending along the external side, follows different electromagnetic patterns (for example the wires are more rarefied at the exterior in comparison to those passing through the hole). The two dynamical uneven behaviors could mimic a sort of 'swimming' within the omnipresent electromagnetic vacuum background. Similar considerations can be done regarding the behavior of the magnetic field, trapped inside the ring along closed orbits.

Finally, unconventional considerations about mass and gravitation have been put forth in [12], section 2.6. They could help to solve the riddle.

5 Realization of the device

We built the ring according to the following procedure. By 3D printing we created two empty semi-rings (see Fig. 4) made of PLA. One of the two parts holds a circular copper wire that will be connected to ground. The proportions are approximately those shown in Fig. 2, and the external diameter is about 11 cm. Both parts have been filled with epoxy resin (relative dielectric constant between 2 and 3) and then glued together.

Figure 4: *Printed support of the ring (left), relative to the bottom part. The internal copper loop, to be connected to ground through a small radial conductor, is visible. On the right, we can see the two parts assembled.*

Successively, as in a toroidal solenoid, the ring has been wound by two sets of windings. According to Fig. 5, they form two independent circuits. These are interlaced and wound following the same chirality. Here, the parameters that may vary are:

- The number of turns in each winding
- The width of the wires
- The chirality

In our case there are 65 turns for each wire. The final result can be seen in Fig. 6.

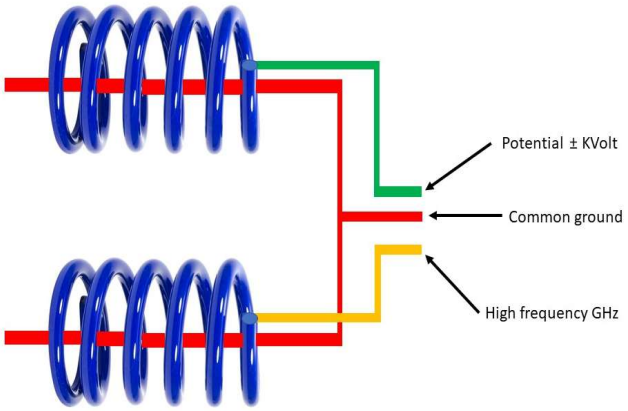

Figure 5: *Electric scheme*

Figure 6: *Final look of the ring.*

The endpoint of one of the two wires is connected to the signal of the RF source, being the ground connected to the central wire inside the ring. The other endpoint is kept floating. The second wire will be connected to a high-voltage generator, with the aim of creating a capacitor having the other pole connected to the central grounded wire. This allows for the development of an internal stationary electric field that would provide a constant value of ρ, as a function of the dielectric features of the material composing the ring.

6 The experiment

In order to measure the generated thrust we used a balance. Several attempts of using electronic tools were done, as also described in Section 7, until we realized that the interference between RF, high voltage electric fields, and measurement device, would have somehow affected the experiment. Therefore, we opted for a pure mechanical instrument, and used an old Mettler B5C1000 Laboratory Scale Analytical Balance Machine, that can support masses up to 1 Kg and can appreciate differences up to $100\mu g$, via an optical nonius. Together with a plastic support, our device has a total mass of about 370 g (see Fig. 7).

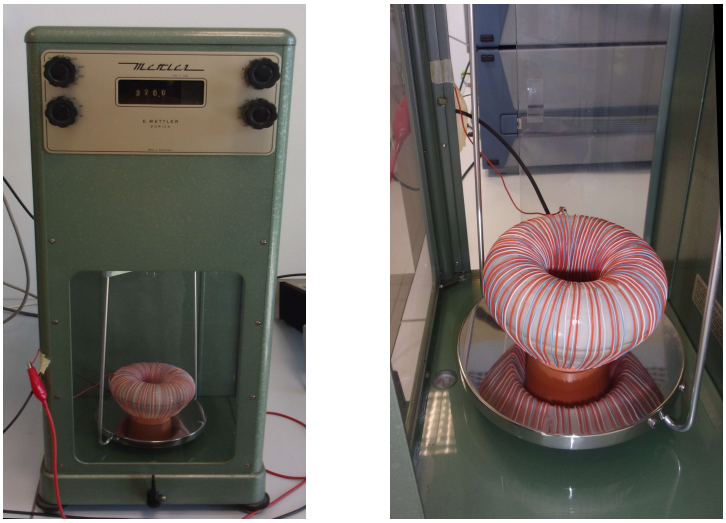

Figure 7: *The device on the plate of the balance machine.*

As a frequency generator we used a Rhode & Schwarz SWM02 which provides frequencies from 0.01 up to 18 GHz. The maximum power output is 12 dBm,

equal to 15.85 mW, while most of the experiments were conducted at 5 dBm, equal to 3.16 mW. The signal passes through a 10 W amplifier, supplied at 12 Volts. The high-voltage DC generator is a Keithley 2410 1100V SourceMeter. The current fed through the circuit is negligible, besides the transitory one, necessary to charge the capacitor consisting of the dielectric material separating the inner loop and one of the two external wires (compare with the scheme of Fig. 5). This produces a value of $\rho \neq 0$ inside the ring, that can be either positive or negative depending on the polarity of the applied voltage.

At frequencies between 913–940 MHz the balance shows consistent and systematic variations of the weight of the EMT. This range is compatible with the size of the device, according to an information that circulates at speeds of the order of that of light. In particular, the EMT was tested in several conditions, varying the RF frequency and power, the DC bias, the orientation of the ring with respect to the vertical axis (up-down or down-up, relatively to the scheme of Fig. 2).

Figure 8 shows examples of the results obtained in the experiments we performed by keeping fixed a value of DC bias and repeatedly switching on/off the RF power, every 10 seconds approximately. A mass change slightly below 1 mg is observed, for a maximum RF power not greater than 10 Watts. The effect of DC bias is also evaluated (Fig. 9), while the RF is kept powering the EMT.

The figures of merit are: a mass variation up to the order of 1×10^{-3} grams, corresponding to a gravitational force of 9.81 mN and a weight variation of approximately $2.7 \times 10^{-5} M$ N/Kg, where M is the mass of the EMT. This would correspond to a maximum efficiency of approximately 980 μ N/W. More concise figures are reported in Table 1. Reversing the orientation of the ring causes a change in the sign of the exerted force, and therefore in a weight loss, instead of a weight gain.

In conclusion, the following facts have been checked:

- The effect is systematic. It clearly appears and disappears by switching the RF power on and off. There is a slight viscous delay, related to the stabilization of the mechanical balance. A linear drift during the measurement is sometimes observed, probably due to temperature variations in the lab and instrumentation.

- The outcome strictly depends on the frequency. Reasonably, this is in relation with the resonance properties of the device. We did not check systematically the full range of frequencies, mainly because the amplifier was not supporting a large band.

- The strength of the outcome is proportional to the power applied. Without the amplifier the effect is hindered.

- The phenomenon is also observed without applying the high-voltage component. We observed a marginal improvement of the performance applying a potential of ± 1 kV (see Fig. 9).

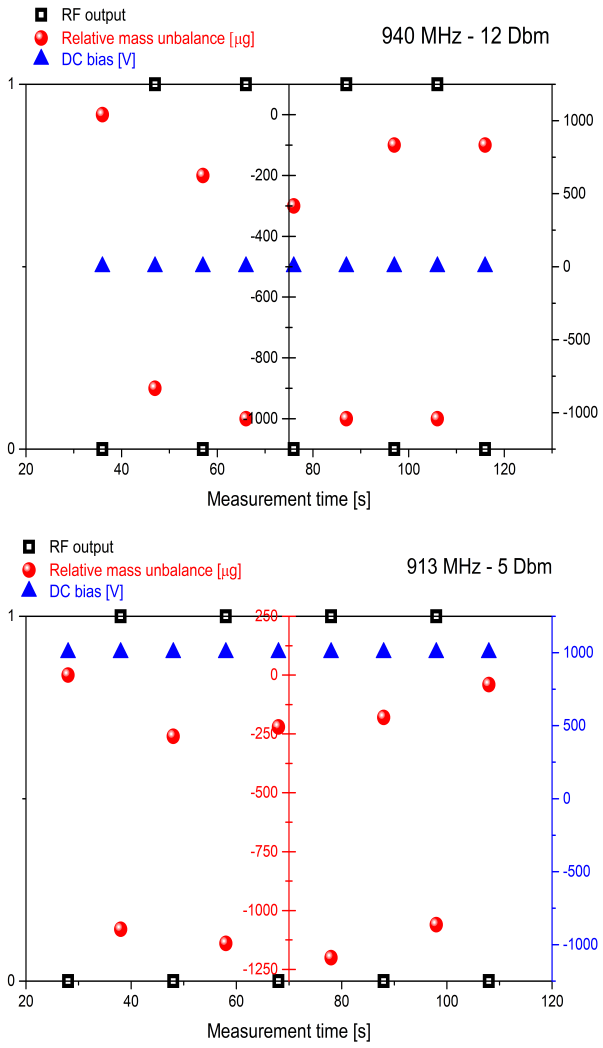

Figure 8: *Outcomes relative to two typical experiments performed while applying the RF field and a DC bias. The RF source is switched on and off periodically, approximately every 10 seconds of acquisition (black open squares: '1' represents the device on, '0' represents the device off), at the frequency and power indicated in the top right inset. The DC bias is set at a fixed value (blue triangles). The balance readings are converted into a relative variation scale by taking as zero the initial value (red circles), and eventually removing the small linear drift that sometimes can be found, presumably due to heating/cooling phenomena during the day. The measure at 940 MHz was performed orienting the EMT as shown in Fig. 2, while the one at 913 MHz was performed by reversing the orientation.*

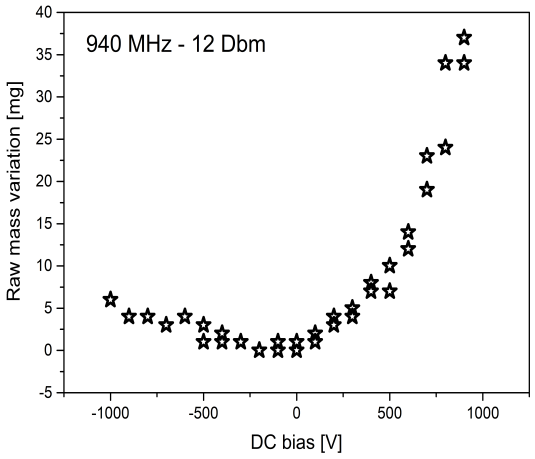

Figure 9: *Effect of the high voltage DC bias on the mass variations, while the RF field is kept on at the frequency and power indicated in the inset. Here the device is oriented as in Fig. 2. The voltage has been varied from -1 KVolt to 1 KVolt and backwards, with steps of 100 Volts. The indication of raw mass variation is referred to the fact that data is untreated to compensate any eventual drift.*

Frequency	Power	DC bias	Device orientation	Mass variation
913	5	0	UP	400 ± 50
913	5	99.95	UP	400 ± 100
913	5	250	UP	450 ± 100
913	5	1000	UP	400 ± 100
913	5	0	DOWN	-700 ± 200
913	5	1000	DOWN	-900 ± 100
940	5	0	DOWN	-600 ± 150
940	12	0	UP	-800 ± 100

Table 1: *Absolute mass change (positive = gain, negative = loss) as a function of the electromagnetic fields submitted to the device. The RF frequency is expressed in MHz, the power in dBm, the DC bias in Volts. The label UP says that the device is oriented as in Fig. 2, whereas DOWN indicates the opposite orientation. Masses and their standard deviations are expressed in μg. We recall that the device has a mass of about 370 g.*

- Applying the high-voltage without the high-frequency signal does not produce any result, as expected.
- The direction of the thrust depends on the verse of orientation of the device, and points towards the bottom as shown in Fig. 3. This is the most important property, which validates the whole experiment.

7 A bit of history and acknowledgments

Soon after the publication of the book [9] (based on the preliminary partial version [16]), a rough prototype was built (see Fig. 10). The electron model introduced in [9], section 5.3 (and successively reexamined in [12], Appendix H) inspired the realization of such a ring-shaped device, having a wiring formed by 208 coils.

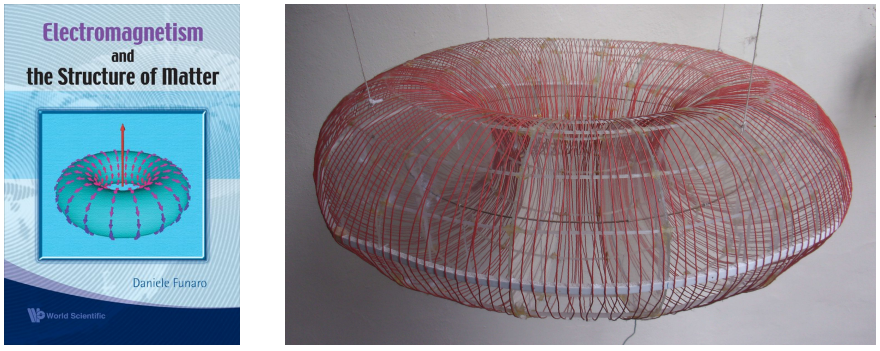

Figure 10: *The cover of the book and an archaic version of the ring.*

The idea is that time-varying electric fields can autonomously create regions where the divergence ρ is different from zero (see for instance the explanation given in [17] in the case of a pulsating charge). This activates the pressure term p in (3.2) with the consequent generation of Newtonian-like forces. The size of the ring (total diameter around 70 cm) was decided depending on the frequency generator available at that time, working at the frequency of about 1GHz. Thanks go to Alfredo Currado for some clarifying theoretical discussions. The lack of adequate instrumentation and the absence of an internal solid dielectric (unessential in principle, but necessary to achieve realistic outcomes) did not allow for the observation of appreciable effects. A possible asymmetry of the device was not taken into consideration. At that time, the purpose was not to get directional thrust, but to create a sort of very mild gravitational screening.

This aspect was also suggested by further observations (as successively reported in [12], p. 58). Due to practical impediments this project was abandoned.

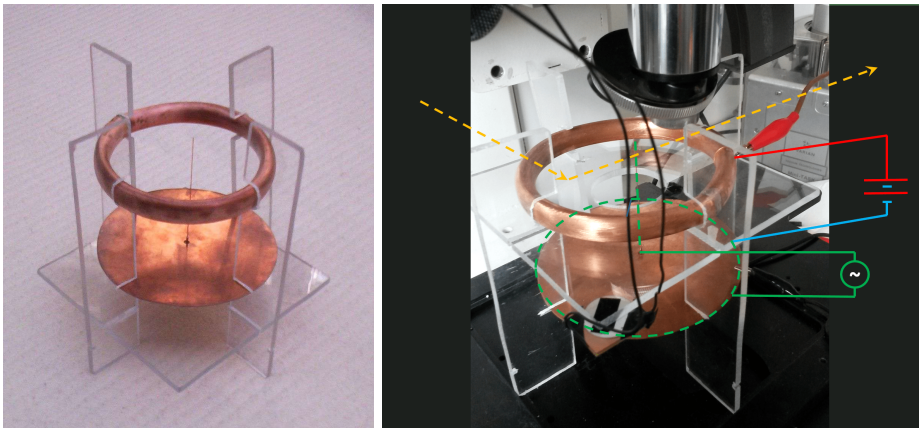

Figure 11: *Left: the device tested in 2014. Right: device under test and labelling to describe how the measurement was conducted. The acrylate transparent structure is used to keep in position the ring and the RF antenna on the one side, and to provide a stable horizontal surface where the cantilever is positioned, to explore the pressure effects. The yellow arrows represent the laser beam directed to the cantilever and reflected towards the four quadrant photodetector. Red and blue lines represent the high voltage connection scheme (the ring on the one side, the copper dish on the other), while green lines represent the RF connection scheme (the central copper wire and the dish). A chip with silicon cantilever was positioned in correspondence with the point of reflection of the laser beam, centered using the microscope objective seen on top of the picture.*

Another experiment was attempted in 2014 at the Physics Department of Politecnico di Torino. To this regard, we would like to thank Marco Crepaldi (Istituto Italiano di Tecnologia, Genova) and Carlo Ricciardi (Dipartimento Scienza Applicata e Tecnologia, Politecnico di Torino) for their kind support. In this new device (Fig. 10), an electromagnetic wave is generated by a quarter-wavelength dipole antenna. A copper ring is connected to a high voltage source (up to 10 kV). The aim was to let the wave circulate around the ring along closed patterns, so generating mechanical pressure (see also the computational results in [18]). For some theoretical guesses, we expected higher pressure than the classical electromagnetic one, which is known to be extremely mild. In the light of the experiences here described in Section 6, that idea looks now very naive. The forces were measured through the continuous monitoring of the resonance of a silicon cantilever, amplified by the deflection of a laser beam that

was focused on the reflecting surface of the cantilever itself, and collected by a four quadrant photodiode. When the forces mediated by the emitting device act on the cantilever, a variation of the resonance frequency is expected. The test failed because an interference between the electromagnetic wave and the solid state laser instrument was observed, producing artifacts. This is also why, in the experiments of Section 6, we opted for a purely mechanical balance.

The possibility of introducing a dielectric was taken into consideration years later. A material with a high dielectric constant, at the operational frequencies of the experiment, reinforces the density ρ in (3.2) and slows down the speed of transfer of electrodynamic information, allowing for the use of smaller objects within an established frequency range. The successful test discussed in these pages is the result of the help offered by various people of Dipartimento di Scienze Chimiche e Geologiche and the Dipartimento di Ingegneria 'Enzo Ferrari' of the Università di Modena e Reggio Emilia. In particular, we would like to thank Andrea Marchetti and Claudio Fontanesi for providing the laboratory instrumentation, Francesco Gherardini and Enrico Dalpadulo for the 3D printing of the ring, Lorenzo Tassi for the filling with epoxy resin, Moreno Maini for some preliminary electric measures on the device.

8 Conclusions

An EMT apparatus has been designed and experimented with success. It is based on a ring geometry and responds to the combined effect of high-frequency signals and stationary high voltage. The impact on the mass M of the body amounts to a variation of approximately $\pm 2.7 \times 10^{-5} M$ N/Kg, corresponding in our case to an applied force of 980 $\mu N/W$, for a power of approximately 10 Watts. More thrust is expected by injecting additional power. There are wide margins of improvements by playing on the geometry and the wiring of the prototype.

In apparent violation of the momentum conservation principle, the device can be used in all applications where, in absence of moving parts, magnets or external fueling, it is necessary to impart acceleration to a frame by means of an electromagnetic input. This phenomenon can be of fundamental importance in many engineering applications, as for instance in the development of new space propulsion units.

Authors Contributions

Funaro: *conceptualization, theoretical formalization, design, assembly of the components, arrangement and supervision of experiments, first draft of the paper and editing of the final version.* Chiolerio: *technical discussion, performing experiments and data analysis, public relations, contacts, editing of the final version of the paper.*

References

[1] Shawyer R. J. (2001), Digitally controlled beam former for a spacecraft, USP 5543801.

[2] Shawyer R. J., www.emdrive.com

[3] Milonni P. W. (1993), *The Quantum Vacuum: An Introduction to Quantum Electrodynamics*, Academic Press.

[4] Cornille P. (2004), *Advanced Electromagnetism and Vacuum Physics*, SCCP, Vol. 21, World Scientific.

[5] Meis C. (2017), *Light and Vacuum*, 2nd ed., World Scientific.

[6] Casimir H. B. G. (1948), On the attraction between two perfectly conducting plates, Proc. Kon. Nederland. Akad. Wetensch., **B51**, 793.

[7] Canning F. X., Melcher C., Winet E. (2004), Asymmetrical capacitors for propulsion, NASA report: CR-2004-213312.

[8] Bahder B., Fazi C. (2002), Force on an asymmetric capacitor, arXiv:physics/ 0211001v2.

[9] Funaro D. (2008), *Electromagnetism and the Structure of Matter*, World Scientific.

[10] Funaro D. (2014), Trapping electromagnetic solitons in cylinders, Math. Model. Anal., **19**, 1, 44-51.

[11] Funaro D. (2018), High frequency electrical oscillations in cavities, Math. Model. Anal., **23**, 3, 345-358.

[12] Funaro D. (2019), *From Photons to Atoms, The Electromagnetic Nature of Matter*, World Scientific.

[13] Funaro D. (2020), Electromagnetic waves in annular regions, Appl. Sci., **10**, 5, 1780.

[14] Chinosi C., Della Croce L., Funaro D. (2010), Rotating electromagnetic waves in toroid shaped regions, Int. J. Modern Phys. C, **21**, 1, 11-32.

[15] Shariff K., Leonard A. (1992), Vortex rings, Annual Rev. Fluid Mech., **24**, 235.

[16] Funaro D. (2005), A full review of the theory of electromagnetism, arXiv:0505068.

[17] Funaro D. (2022), The space-time outside a pulsating charged sphere, Appl. Sci., **12**, 14, 7290.

[18] Funaro D., Kashdan E. (2015), Simulation of electromagnetic scattering with stationary or accelerating targets, Int. J. Modern Phys. C, **26**, 7, 1-16.